ELSEVIER

Nanomedicine: Nanotechnology, Biology, and Medicine
48 (2023) 102656

nanomedicine
Nanotechnology, Biology, and Medicine

nanomedjournal.com

Intraperitoneal administration of cabazitaxel-loaded nanoparticles in peritoneal metastasis models

Astrid Hyldbakk, M.Sc.[a,b,*,1], Karianne Giller Fleten, PhD[c,d,1], Sofie Snipstad, PhD[a,b,e], Andreas K.O. Åslund, PhD[a], Catharina de Lange Davies, PhD[b], Kjersti Flatmark, MD, PhD[c,d,f,1], Yrr Mørch, PhD[a,1]

[a]*Department of Biotechnology and Nanomedicine, SINTEF Industry, Trondheim, Norway*
[b]*Department of Physics, Norwegian University of Science and Technology (NTNU), Trondheim, Norway*
[c]*Department of Tumor Biology, Institute for Cancer Research, Norwegian Radium Hospital, Oslo University Hospital, Oslo, Norway*
[d]*Faculty of Medicine, Institute of Clinical Medicine, University of Oslo, Oslo, Norway*
[e]*Cancer Clinic, St. Olav's Hospital, Trondheim, Norway*
[f]*Department of Gastroenterological Surgery, Norwegian Radium Hospital, Oslo University Hospital, Oslo, Norway*

Revised 20 December 2022

Abstract

Colorectal and ovarian cancers frequently develop peritoneal metastases with few treatment options. Intraperitoneal chemotherapy has shown promising therapeutic effects, but is limited by rapid drug clearance and systemic toxicity. We therefore encapsulated the cabazitaxel taxane in poly(alkyl cyanoacrylate) (PACA) nanoparticles (NPs), designed to improve intraperitoneal delivery. Toxicity of free and encapsulated cabazitaxel was investigated in rats by monitoring clinical signs, organ weight and blood hematological and biochemical parameters. Pharmacokinetics, biodistribution and treatment response were evaluated in mice. Biodistribution was investigated by measuring both cabazitaxel and the 2-ethylbutanol NP degradation product. Drug encapsulation was shown to increase intraperitoneal drug retention, leading to prolonged intraperitoneal drug residence time and higher drug concentrations in peritoneal tumors. As a result, encapsulation of cabazitaxel improved the treatment response in two *in vivo* models bearing intraperitoneal tumors. Together, these observations indicate a strong therapeutic potential of NP-based cabazitaxel encapsulation as a novel treatment for peritoneal metastases.
© 2023 The Authors. Published by Elsevier Inc. This is an open access article under the CC BY license (http://creativecommons.org/licenses/by/4.0/).

Keywords: Peritoneal metastases; Intraperitoneal administration; Poly(alkyl cyanoacrylate) nanoparticles; Cabazitaxel; Drug delivery

Background

Cancers originating in the abdominal organs, such as the ovaries and the colorectum, often give rise to metastases in the peritoneal cavity. Peritoneal metastases (PM) do typically not cause clear clinical symptoms, which limits early detection of the disease and leads to high numbers of late-stage cancer diagnoses and poor patient prognosis. Current treatment strategies involve cytoreductive surgery (CRS) followed by systemic chemotherapy or hyperthermic intraperitoneal chemotherapy (HIPEC). Unfortunately, only a subgroup of patients is eligible for this treatment and the majority of patients receiving this treatment will experience relapse. Patients with PM respond poorly to systemic chemotherapy, and intraperitoneal administration of cytotoxic drugs has therefore been given to achieve high local drug concentrations.[1–3] However, these drugs are rapidly cleared from the peritoneum, leading to short exposure times. By encapsulating drugs in nanoparticles (NPs) it is possible to slow down systemic adsorption and prolong the peritoneal residence time.[4–6] Due to their physicochemical characteristics,

* Corresponding author at: Department of Biotechnology and Nanomedicine, SINTEF Industry, Kjemihallen, Sem Sælands Vei 2a, 7034 Trondheim, Norway.
E-mail addresses: astrid.hyldbakk@sintef.no (A. Hyldbakk), karianne.giller.fleten@rr-research.no (K.G. Fleten), sofie.snipstad@sintef.no (S. Snipstad), andreas.aaslund@sintef.no (A.K.O. Åslund), catharina.davies@ntnu.no (C.L. Davies), kjersti.flatmark@rr-research.no (K. Flatmark), yrr.morch@nadeno.com (Y. Mørch).
[1] Contributed equally.

https://doi.org/10.1016/j.nano.2023.102656
1549-9634/© 2023 The Authors. Published by Elsevier Inc. This is an open access article under the CC BY license (http://creativecommons.org/licenses/by/4.0/

nanomedicines are preferentially retained in the peritoneal cavity where the drug is released to exert its cytotoxic effect, while systemic toxicity is reduced. NPs are also shown to specifically accumulate in tumor tissue,[7–9] and have been suggested as perioperative treatment after HIPEC for PM patients.[10]

Poly(alkyl cyanoacrylate) (PACA) based materials, mainly known for their extensive use as surgical glues and tissue adhesives, have shown great promise as platforms for drug delivery, based on their biocompatible and biodegradable cyanoacrylate polymers.[11,12] Its chemical tunability allows for encapsulation of drugs of different chemical nature and the functionality can be customized for specific applications, *e.g.* by adding surface ligands. PACA has reached several late-stage clinical trials, including the phase III clinical trial RELIVE for treatment of liver cancer with doxorubicin-loaded poly(etylbutyl cyanoacrylate) (PEBCA) NPs.[13] In this study, the NP-based treatment showed a favorable efficacy and tolerability profile, but no significant differences could be observed in overall survival when compared to best standard of care (standard systemic anticancer therapy according to the center's practice).

We have previously reported promising therapeutic effects in mice of PEBCA-NPs encapsulating the cytotoxic drug cabazitaxel (CAB).[14–16] CAB is a microtubule inhibitor approved for treatment of metastatic hormone-refractory prostate cancer, currently used under the trade name Jevtana®. This is an attractive candidate for PACA encapsulation, as encapsulation may enable reduction of severe off-target toxicity and increase tumor accumulation.[17] Based on this, we have developed the PACAB NP product (PEBCA NPs encapsulating the CAB drug), specifically designed for peritoneal tumor accumulation and retention. In the present study, the overall aim was to study the potential of PACAB as a novel treatment strategy for PM patients. The *in vivo* profile of PACAB was compared to that of free (un-encapsulated) CAB, with the focus on toxicity, pharmacokinetics, biodistribution and therapeutic efficacy.

In the study presented here, the toxicity profile of PACAB, empty PACA NPs and free CAB drug was investigated after ip injection in rats. In order to follow the *in vivo* fate of CAB, liquid chromatography tandem mass spectrometry (LC–MS/MS) was used to quantitate CAB in blood and tissue samples following ip injection of PACAB and free drug, and intravenous (iv) injection of PACAB. LC–MS/MS allows for specific and sensitive label-free detection of the therapeutic drug, enabling pharmacokinetic and biodistribution studies on the nanomedicine without introducing a fluorescent model drug.

Despite a relatively high number of published studies on biodistribution of NP-systems after ip injection, very few include data showing the *in vivo* fate of the particle material. In this study, a novel gas chromatography mass spectrometry (GC–MS)-based method was developed to study the biodistribution of the PACAB NP material. This was achieved by sensitive detection of 2-ethylbutanol (2-EB), a specific PEBCA degradation product released upon sample hydrolysis.

Finally, the therapeutic effect after ip injection of PACAB and free drug was compared in two *in vivo* models mimicking peritoneal metastasis; an orthotopic mucinous patient-derived xenograft model and an ovarian cancer cell line injected ip.

Materials and methods

Formulation of CAB and PACAB

The cytostatic drug CAB was administered either as a micelle formulation, similar to the clinical Jevtana® formulation, or encapsulated in poly(2-ethylbutyl cyanoacrylate) (PEBCA) NPs. To prepare the micelle formulation, CAB dry powder (>98 % purity; Biochempartner Co. Ltd., Wuhan, China) was dissolved in polysorbate 80 (Sigma-Aldrich, St. Louis, MO, USA) to 40 mg CAB/mL. This was done by mixing 60 mg drug with 1590 mg Polysorbate 80 (1.06 g/mL) by magnetic stirring overnight (room temperature) until a completely clear solution was obtained. The micelles have been shown to have a mean diameter of about 10 nm in aqueous solution.[18] Directly before injection into the animal, the stock solution was diluted with 13 % (v/v) ethanol to a working solution of 10 mg/mL CAB, and further used to prepare an injection solution in 0.9 % (w/v) NaCl.

PEGylated PEBCA NPs were synthesized using a miniemulsion polymerization technique, as previously described.[16] Briefly, an oil phase, containing 2-ethylbutyl cyanoacrylate (EBCA, Cuantum Medical Cosmetics, Bellaterra, Spain) and the co-stabilizer Miglyol® 812 (1.9 % (w/w), Cremer Oleo GmbH & Co. KG, Hamburg, Germany) was mixed with a water phase consisting of the non-ionic PEG stabilizers Brij® L23 (6.8 mM, Sigma-Aldrich) and Kolliphor® HS 15 (8.7 mM, Sigma-Aldrich) in 0.1 M HCl. Compounds to be encapsulated within the PACA nanoparticles (NR668, 0.2 % (w/w), modified Nile Red, custom synthesis[19] or CAB, 10 % (w/w)) were added to the oil phase prior to mixing. The emulsions were sonicated, adjusted to pH 5 (0.1 M and 1 M NaOH) and dialyzed (12–14 kDa Molecular Weight Cut-Off (MWCO)) before size, polydispersity index (PDI) and Zeta-potential were measured by a Zetasizer Nano ZS (Malvern Instruments, Malvern, UK) in 0.01 M phosphate buffer, pH 7.

CAB quantification by LC–MS/MS

Drug loading was measured by extracting CAB from the particles by dissolving them in acetone. CAB drug content was quantified by LC–MS/MS (Agilent 1290 HPLC system coupled to an Agilent 6495 triple quadrupole mass spectrometer, Agilent Technologies, Santa Clara, CA, USA), as previously described.[14]

2-EB quantification by GC–MS

The ethylbutyl alkyl groups on the PEBCA polymer chain are released as free 2-ethylbutanol (2-EB) alcohols upon hydrolysis. This can be exploited to quantify the polymeric material in different samples. 2-EB reference standards (E14659, Sigma-Aldrich) were prepared by acetone dilution and used for calibration. Samples were analyzed with an Agilent 7890B chromatograph equipped with an Agilent DB-WAX column (122-7032) coupled to an Agilent G7039A MS. 1 μL sample was injected in split mode (1:10) and run isothermally at 40 °C for 4 min before initiating a temperature gradient of 10 °C/min until 250 °C. Total run time per sample was 27.5 min. The internal standard 1-hexanol (H13303, Sigma-Aldrich) was added to a final concentration of 5 μg/mL to correct for possible matrix effects.

In vitro viability

The human ovarian cancer cell line B76 was a kind gift from C. Marth (Innsbruck Medical University, Innsbruck, Austria)[20] and was established from a patient with serous adenocarcinoma ovarian cancer. The cell line was transduced with a retroviral vector (lmg*) containing a GFP-luc construct as described previously.[21] The cells were grown in RPMI-1640 (Sigma-Aldrich), supplemented with 10 % fetal bovine serum (Sigma-Aldrich) and 1 mM L-glutamine (Sigma-Aldrich) at 37 °C with 5 % CO_2. The mesothelial cell line LP9 was purchased from Coriell Institute for Medical Research (Cat no. AG07086, Camden, NJ, USA) and cultivated in Medium 199 (Sigma-Aldrich)/MCDB110 (US biological Life Sciences, Salem, MA, USA) mixed 1:1 with 1 mM L-glutamine, 15 % fetal bovine serum, 10 ng/mL epidermal growth factor, 0.4 μg/mL hydrocortisone and 1 % penicillin/streptomycin (All supplements from Sigma-Aldrich) at 37 °C with 5 % CO_2. To evaluate response to CAB, PACAB or empty NPs, B76 (15,000 cells) or LP9 (1875 cells) were seeded in 96-well plates. Free CAB, PACAB or empty PACA NPs (0.0001, 0.001 or 0.01 μg CAB/mL, corresponding to 0.001, 0.01 or 0.1 μg NPs/mL) were added after 24 h. Cell survival was evaluated using CellTiter-Glo (CTG) (Promega, Madison, WI, USA) 72 h later.

In vivo experiments

All procedures and experiments involving animals were approved by the Norwegian Food Safety Authority and conducted according to the recommendations of the European Laboratory Animals Science Association (FELASA). The ethical approval numbers are 25354 (toxicity study in rats), 24189 (biodistribution study in healthy rats), 18209 (treatment of PMCA-3 tumors) and 28853 (biodistribution study in tumor bearing mice and treatment of B76 tumors). Animals were kept under specific pathogen free conditions, with constant temperature and relative humidity. Food and water were supplied *ad libitum*.

Toxicity profiling in rats

Female Sprague Dawley rats (Janvier Labs, Le Genest-Saint-Isle, France) were purchased at 10 weeks of age and used at body weight of approx. 300 g. Toxicity effects following a single ip injection of empty PACA NPs, PACAB or free CAB were studied in healthy rats (n = 4 per timepoint). CAB were given as a dose of 7.5 mg CAB/kg, PACAB as 7.5 mg CAB/kg (corresponding to 75 mg PACA NPs/kg) and a comparable amount of empty NPs (75 mg PACA NPs/kg) was used as control. The 7.5 mg/kg CAB dose was chosen based on previous efficacy studies in mice using 7.5–15 mg/kg.[14,16] The highest dose was converted from mice to rats by a conversion factor of 0.5.[22] This corresponded to injection volumes of 550–680 μL. An equivalent volume of 0.9 % NaCl per rat body weight was used as negative control. Before injection, animals were anesthetized with isoflurane (2–3 %, Baxter, Deerfield, IL, USA), and morphine analgesia (1 mg/kg) was administered subcutaneously directly after injection to avoid abdominal constriction responses.

All rats were monitored regularly for body weight and health status (such as activity level, grooming, behavior and clinical symptoms) and were euthanized by exsanguination under full anesthesia at the scientific endpoint or at humane endpoints if the body weight decreased >15 %. Blood and tissue samples (brain, liver, spleen, kidneys and heart) were harvested at 4 h, 3 d and 10 d post-injection and weighed immediately after dissection.

Blood samples were taken during anesthesia by terminal cardiac puncture in tubes coated with EDTA (Sarstedt Microvette® K3 EDTA, 500 μL, Sarstedt, Nümbrecht, Germany) for blood hematology and in tubes with Clotting Activator (Sarstedt Microvette® Clotting Activator/Serum, 500 μL) for determination of clinical chemistry parameters. The EDTA tubes were gently inverted 8–10 times to ensure proper mixing with the coagulant, and stored at 4 °C until they were analyzed for hematological parameters within 24 h. The Clotting Activator serum tubes were left to clot in an upright position at room temperature for 1 h, before the serum was separated from the blood cells by centrifugation (5 min, 10.000 rcf, room temperature). The serum was transferred to new, empty tubes, and kept frozen (−80 °C) until clinical chemistry analysis.

Biodistribution and pharmacokinetics studies in mice

For biodistribution studies using fluorescence, locally bred 6–8-weeks old female athymic foxn 1^{nu} mice were used. PACA NPs labelled with NR668 (143 mg PACA NPs/kg) were injected (200–250 μL) either ip or iv. For biodistribution studies of CAB and 2-EB, female immunocompetent balb/c and athymic nude mice (Janvier Labs) were purchased at 8 weeks of age and used at body weight of approx. 20 g. Mice were given a single dose of 6 mg/kg CAB either as free drug ip, PACAB ip or iv (6 mg CAB/kg, 56 mg PACA NPs/kg), or a comparable volume of saline as control (60 μL). The tail vein was used for iv injections, while ip injections were made in the lower right abdominal quadrant. All mice were monitored regularly by assessment of body weight and health status. At given timepoints (Table 1), blood samples were withdrawn either by puncture of the lateral saphenous vein, or by terminal blood sampling after decapitation. Blood samples were collected in EDTA tubes (Sarstedt Microvette® CB 300 K2 EDTA, 300 μL), thoroughly mixed, and kept frozen (−20 °C) until CAB analysis by LC–MS/MS as described above. All procedures regarding injection, blood sampling and euthanization were performed under isoflurane anesthesia (2–3 %).

Table 1
Biodistribution sampling points and number of animals in each group.

Euthanasia	Blood sampling	Number of animals			
		CAB ip	PACAB ip	PACAB iv	Control ip
1 h	1 h	4	4	4	1
1 day	iv: 30 min/ip: 90 min, 1 day	4	4	4	1
2 days	iv: 1 min/ip: 5 min, 2 days	4	4	4	1
4 days	iv: 10 min/ip: 15 min, 4 days	4	4	4	1
7 days	4 h, 7 days	4	4	4	1
35 days	2 h, 35 days	4	4	4	1

Biodistribution in B76 tumor bearing animals was studied in locally bred 6–8-weeks old female athymic foxn 1^{nu} mice injected ip with B76-GFP/luciferase cells (2.5×10^6 cells in 500 μL RPMI medium). Treatment was administered on day 4 (tumors < 2 mm) after injection. Mice were randomly assigned to treatment with free drug (6 mg/kg) or PACAB (6 mg/kg CAB, 60 mg PACAB NPs/kg) (10 mice in each group) and euthanized 2 h after administration of treatment.

Tissue samples (kidneys, liver, spleen and an approx. 2 × 1 cm section of the parietal peritoneum, excised from the ip injection site) were harvested from all animals. The samples were weighed and analyzed to quantify CAB and the PEBCA polymer (2-EB) content. This was done after tissue homogenization performed by the enzymatic digestion protocol developed as described in Fusser et al.[14] In order to release all 2-EB, the PEBCA polymers in the sample were fully hydrolyzed. This was performed by diluting homogenized tissue samples 1 + 1 in 0.1 M NaOH and heating to 40 °C at gentle stirring for 24 h. Stability of 2-EB under these conditions was verified by including 2-EB controls in the hydrolyzation step. The hydrolyzed samples were diluted 10× in acetone before centrifugation (14,000 ×*g*, 10 min) was performed to precipitate proteins and other macromolecules.

Therapeutic efficacy in vivo

Therapeutic efficacy following injection of control, free drug and PACAB was studied in B76 and PMCA-3 models. Locally bred 6–8 weeks old female athymic foxn 1^{nu} mice were injected ip with B76-GFP/luciferase cells (as described above) or 200 μL mucinous ascites from the model PMCA-3. PMCA-3 was established from a patient with pseudomyxoma peritonei (PMP) by implantation of tumor tissue in the peritoneal cavity of mice collected at the time of CRS-HIPEC, and is classified as a high grade PMP with signet ring cell differentiation (previously described).[23] For both models, the aim was to mimic the state of the peritoneal cavity after cytoreductive surgery, *i.e.* to start treatment with a minimal remaining intraperitoneal tumor burden. For B76 tumors, treatment was administered on day 4 (tumors < 2 mm), while for PMCA-3, treatment was administered the day after injection. Mice were randomly assigned to treatment groups of six mice, and given 200–250 μL of saline with 1.2 % EtOH, CAB (6 and/or 15 mg/kg) or PACAB ip (6 and/or 15 mg/kg, corresponding to 58, 116, 144 or 164 mg PACA NPs/kg). The animals were monitored regularly for changes in body weight and health status, and were euthanized by cervical dislocation if abdominal distension occurred, if body weight decrease of >15 % was observed, or on day 100 if no symptoms occurred. One mouse (PMCA-3; PACAB group) was excluded from analyses due to death not related to tumor growth.

Fluorescence and luminescence imaging

Luminescence and fluorescence images were obtained using the *in vivo* imaging system IVIS Spectrum (Perkin Elmer). Sevofluran (3 %) was used for anesthesia during imaging. Fluorescence imaging was performed to visualize distribution of NR668 labelled NPs 1 h after iv and ip injection using excitation/emission spectra of 535/640 nm. Luminescence was used to evaluate tumor growth in mice with B76 cells. Mice were injected with 200 μL luciferin (20 mg/mL; Biosynth, Staad, Switzerland diluted in phosphate buffered saline) ip 10 min before imaging. Both dorsal and ventral images were taken, and the average luminescence of these images was used for calculations. Analyses of the images were performed using Living Image Software (Perkin Elmer).

Magnetic resonance imaging of abdomen

Magnetic resonance imaging (MRI) was performed as previously described,[21] using a 7T MR system (Bruker BioSpin MRI GmbH, Ettlingen, Germany, Software ParaVision 6.0) equipped with a volume T/R resonator with 75/40 mm diameter. To ensure correct placement and location of the abdomen, a fast gradient echo localizer scan was first performed, before a coronal T2-weighted rapid acquisition with relaxation enhancement (RARE) sequence (repetition time = 2 s, echo time = 26.5 ms and echo train length = 8) was used to image the whole abdomen. Slice thickness was 0.7 mm with a slice gap of 0.3 mm, field of view 4 × 3 cm^2 and matrix size 364 × 364.

Data processing and statistical analysis

CAB content was calculated and plotted as a function of time to establish the pharmacokinetic parameters C_{max} (maximum observed drug concentration), t_{max} (time to reach C_{max}) and AUC (area under the curve). This was performed using GraphPad Prism (version 9.2.0 for Windows, GraphPad Software, San Diego, CA, USA). To estimate CAB blood half-life ($t_{1/2}$), log-transformed concentration data was plotted as a function of time. The resulting curves were fitted to a bi-exponential distribution, where the slope of each phase was used to calculate the CAB half-life ($t_{1/2} = \ln(0.5)/\text{slope}$). These calculations were performed by Microsoft Excel (version 2111 for Microsoft 365 MSO, WA, USA).

Statistical analyses were conducted using GraphPad Prism v9 or Microsoft Excel. Survival curves (Kaplan–Meier plot) were compared using log-rank test. Differences in tumor weight were compared using unpaired *t*-test. One-way analysis of variance (ANOVA) with post hoc comparisons by Dunnett's *t*-test was applied on organ-to-brain weight data and blood sample data. In all instances, p-values < 0.05 were considered statistically significant. Mean and standard deviation (SD) are displayed in the various figures.

Results

Characterization of PACA NP formulations

Empty NPs were in the size range of 132–168 nm (diameter, z-average), had a polydispersity index (PDI) below 0.2 and a zeta potential between −3.2 and −4.3 mV. NR668-loaded PACA NPs were 136 nm, had a PDI of 0.17 and a zeta potential of −3.1 mV. PACAB (CAB-loaded PACA NPs) were in the size range of 125–181 nm, had a PDI below 0.3, a zeta potential between −2.5 and −5.8 mV and a CAB content of 9.6–14.2 mg/mL particle

stock suspension. Curves showing size and zeta potential distribution of representative NP batches are presented in Fig. S1. NP surface PEGylation resulted in colloidal stability and no NP aggregation was observed in any of the batches.

In vitro toxicity studies

Before conducting *in vivo* experiments, the PACA NP toxicity was evaluated in two relevant cell lines. The viability of B76 ovarian cancer cells and LP9 mesothelial cells (the cell type that lines the peritoneal cavity) after incubation with 0.0001, 0.001 or 0.01 μg CAB/mL of either free drug or PACAB is shown in Fig. S2. The results show no differences between incubation with free drug and PACAB in any of the cell lines, and at the highest dose of 0.01 μg CAB/mL practically all cells were dead. For a typical PACAB batch with 10 % (w/w) CAB loading, this corresponds to a PACAB dose of 0.0001 mg PACAB/mL. Empty NPs did not reduce cell viability before the NP concentration was increased to 0.1 mg PACAB/mL.

Toxicity profiling in rats

Various parameters, including body and organ weight, animal behavior and clinical signs, hematology and clinical chemistry parameters were monitored in rats after injection of free drug, PACAB, empty NPs and saline control. Injection of PACAB and empty NPs caused an abdominal constriction response, as we observed lateral constriction of the flank abdominal muscles during the first hours after ip injection. This is a common response to irritations in the peritoneal cavity after ip injections.[24] After this observation, all ip injections were performed after subcutaneous injection of morphine analgesia. This response was not observed in the saline control animals or in CAB-treated animals. Injection of free cytostatic drug resulted in a rapid decrease in body weight (Fig. 1). Rats receiving the encapsulated drug formulation also showed reduced body weight, although the signs of toxicity were less prominent. At day 3 after injection, 2 out of 8 PACAB treated animals showed diarrhea and lack of grooming, compared to 6 out of 8 animals injected with free drug. Two animals were euthanized at day 4 (both treated with free drug) and two animals were euthanized at day 7 (one from the PACAB group and one from the free drug group) to ensure humane endpoints. After the 7-day timepoint, clinical signs and animal behavior improved in both CAB treated groups. Injection of empty NPs caused a momentary, but transient weight loss, where all animals quickly regained their initial weights. No animals showed signs of diarrhea or lack of grooming. The saline control animals showed a steady weight increase throughout the whole study period, without any weight loss or clinical signs.

After dissection, the brain, heart, lungs, liver, spleen, and kidneys were weighed, before the organ-to-brain weight ratios were calculated. Only few statistically significant differences from the saline control could be observed (Fig. S3). For the PACAB group, a decrease in liver-to-brain ratio was seen at the 4 h timepoint and a decrease in heart-to-brain ratio was seen at the 10 day timepoint. For the free drug group, significant increases in lung-to-brain, liver-to-brain and spleen-to-brain ratios were seen 10 days after injection. No changes could be observed in the empty NP treatment group.

The effect of administration of empty NPs, free drug and PACAB on hematological and biochemical parameters in blood samples is listed in Tables S1 and S2, respectively. For the empty NP treatment group, an acute and transient increase in the number of neutrophils and monocytes indicated an innate immune response – stronger than the response observed in groups treated with PACAB or free drug. For the PACAB and free drug treatment groups, a general decrease of all types of white blood cell was observed, and the effect was most prominent in the group treated with free drug. In these two CAB treated groups, an acute and transient increase in red blood cell (RBC) count, hemoglobin concentration and hematocrit was observed, before the concentrations decreased and reached levels lower than the saline controls. On the contrary, empty NPs induced an increase in all RBC parameters 10 days after injection. A decrease in the platelet count could be observed for all treatment groups, where the response was more acute and transient in the PACAB and free drug groups.

Analysis of blood clinical chemistry parameters revealed few differences between the treatment groups and the saline controls. Significant changes in the electrolyte balance, creatinine, albumin and urea could be seen for all treatment groups. For the PACAB and free drug groups, a transient decrease could be observed for the alkaline phosphatase enzyme and a transient increase could be observed in glucose levels. Total protein levels were shown to decrease gradually after treatment with PACAB and free drug.

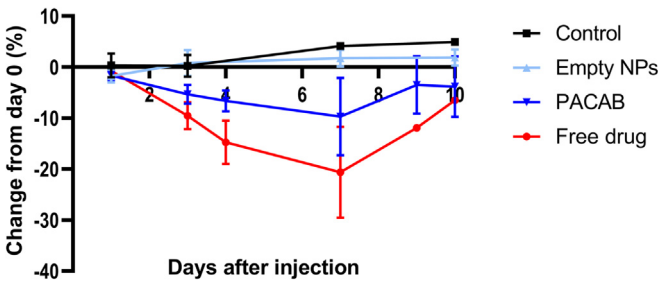

Fig. 1. Rat body weight change after ip injection with free drug (7.5 mg CAB/kg), PACAB (7.5 mg CAB/kg) or empty NPs (data shows mean ± standard deviation). Number of animals at the time points are reduced as animals are euthanized: Day 0–3: 4 Control, 8 Empty NPs, 8 PACAB, 8 Free drug; Day 4–7: 2 Control, 4 Empty NPs, 4 PACAB, 4 Free drug; Day 9–10: 2 Control, 4 Empty NPs, 3 PACAB, 1 Free drug.

Pharmacokinetics and biodistribution of CAB and PACAB NPs in healthy mice

CAB levels in blood and tissue extracts were studied after injection of PACAB and free drug in healthy mice. Pharmacokinetic parameters determined from the blood concentration-time profiles (Fig. S4) showed large differences between the groups (Table 2). Ip administration of PACAB significantly reduced the amount of drug reaching systemic circulation compared to iv administration, illustrated by a 22× reduction in C_{max} and a 3.6× reduction in AUC. Additionally, ip injection postponed t_{max} by 1 h and somewhat prolonged the initial distribution phase. Importantly, CAB encapsulation in PACA NPs was shown to almost halve the C_{max} compared to injection of free drug and to prolong the elimination half-time approximately 10 times.

Biodistribution of PACA NPs was studied by three complementary methods: Whole-animal imaging of PACA-encapsulated NR668, mass spectrometry-based quantification of CAB, and analysis of the NP degradation product 2-EB in tissue extracts. As shown in Fig. 2A, PACA NPs were evenly distributed throughout the entire peritoneal cavity within the first hour after ip injection, with low amounts of fluorescence in the rest of the animal – indicating NP retention in the peritoneal cavity. After iv injection, fluorescent signal could be observed in the entire animal, clearly showing the differences in biodistribution by the different administration methods.

CAB levels were measured in liver, spleen, kidney and peritoneum tissue after different time points from 1 h up to 35 days (840 h). Total CAB tissue exposure, illustrated as AUC values calculated based on CAB concentration-time profiles for the different groups, are shown in Fig. 2B. The corresponding concentration-time curves can be found in Fig. S5A. CAB exposure was significantly higher in all tissues when injected as PACAB compared to free CAB administered by the same route – as much as an 8× increase could be found in peritoneum tissue. PACAB administration by ip *vs* iv routes resulted in comparable CAB exposure levels in liver, spleen and kidney, while iv injection expectedly induced limited exposure in peritoneum.

To study the biodistribution of the NP material, a novel method was developed to detect the PEBCA-specific degradation product 2-ethylbutanol (2-EB) in biological matrices. Tissue samples were hydrolyzed to release 2-EB, before 2-EB was quantitatively analyzed by GC–MS. AUC values are presented in Fig. 2C, and the corresponding concentration-time profiles are to be found in Fig. S5B. Interestingly, 2-EB was found in liver and spleen as late as 35 days post-injection, while CAB was cleared from the same tissues at this time point.

Biodistribution of CAB and PACAB in B76 tumor bearing mice

To study potential CAB tumor accumulation, a follow-up study was performed in B76 tumor bearing mice. The results presented in Fig. 3A show a significant increase in tumor-associated CAB after PACAB injection compared to free CAB, with a 10× increase in mean CAB concentration in tumor tissue 2 h post injection. A significant increase in CAB concentrations in peritoneum, liver and spleen was also observed.

A strong tumor specific association could be seen for the PACA NP material, shown by high concentrations of 2-EB in the tumor tissue, whereas no 2-EB could be found in tissue excised from the peritoneal injection site. 2-EB was also detected in liver and spleen (Fig. 3B).

Therapeutic efficacy

Mice bearing PMCA-3 xenografts developed mucinous ascites and tumor growth between the organs eventually leading to distended abdomen and euthanization to ensure humane endpoints. The growth pattern of the model is shown in Fig. 4A using T2 weighted MRI, where the tumor tissue can be seen as white areas. Control-treated mice had a median survival of 33 days, whereas survival was significantly increased by CAB and PACAB to 56.5 and 76 days, respectively. None of the mice treated with CAB were alive at day 100 when the experiment was terminated, while four mice treated with PACAB were still alive. Of these, two mice showed no sign of tumor and were considered cured (Fig. 4B).

Animals injected with B76 cells rapidly developed extensive tumor growth on all peritoneal surface areas, and in many cases also ascites. Control-treated mice were euthanized between days 27–31 (median survival 29 days), and had 1.45 ± 0.21 g tumor tissue. Empty NP did not significantly affect survival compared to control and the mice were euthanized between days 21–28 (median survival 24 days), but the tumor weight was significantly reduced (0.76 ± 0.40 g, $p = 0.01$) (data not shown). CAB and PACAB strongly inhibited tumor growth and a difference in luminescence compared to the control treated group was observed already at day 10, which was the first imaging time point after treatment. Animals treated with CAB (6 and 15 mg/kg) and

Table 2
Effect of NP encapsulation and administration route on blood pharmacokinetic parameters of CAB in healthy mice (n = 4 animals per group per time point, data shows mean and standard deviation).

	C_{max} (μg/mL)	t_{max} (min)	$t_{1/2}$ distribution (h)	$t_{1/2}$ elimination (h)	AUC (μg/mL * h)
Free drug ip	1.58 ± 0.30	60.0 ± 0	1.1 ± 0.2	7.1 ± 0.4	4.90 ± 0.95
PACAB ip	0.91 ± 0.25[a,b]	67.5 ± 15[a]	8.8 ± 14.0	66.6 ± 13.5[b]	6.55 ± 2.64[a]
PACAB iv	19.30 ± 4.83	1.0 ± 0	2.0 ± 0.6	62.9 ± 10.1	23.49 ± 5.31

C_{max}: maximum concentration, t_{max}: time to C_{max}, $t_{1/2}$ distribution: half-life of the distribution phase (1–4 h), $t_{1/2}$ elimination: half-life of the elimination phase (4–48 h for free drug, 48–168 h for PACAB), AUC: area under the blood concentration-time curve from first to last sampling point.

[a] PACAB ip result significantly different from PACAB iv result.

[b] PACAB ip result significantly different from free drug ip result.

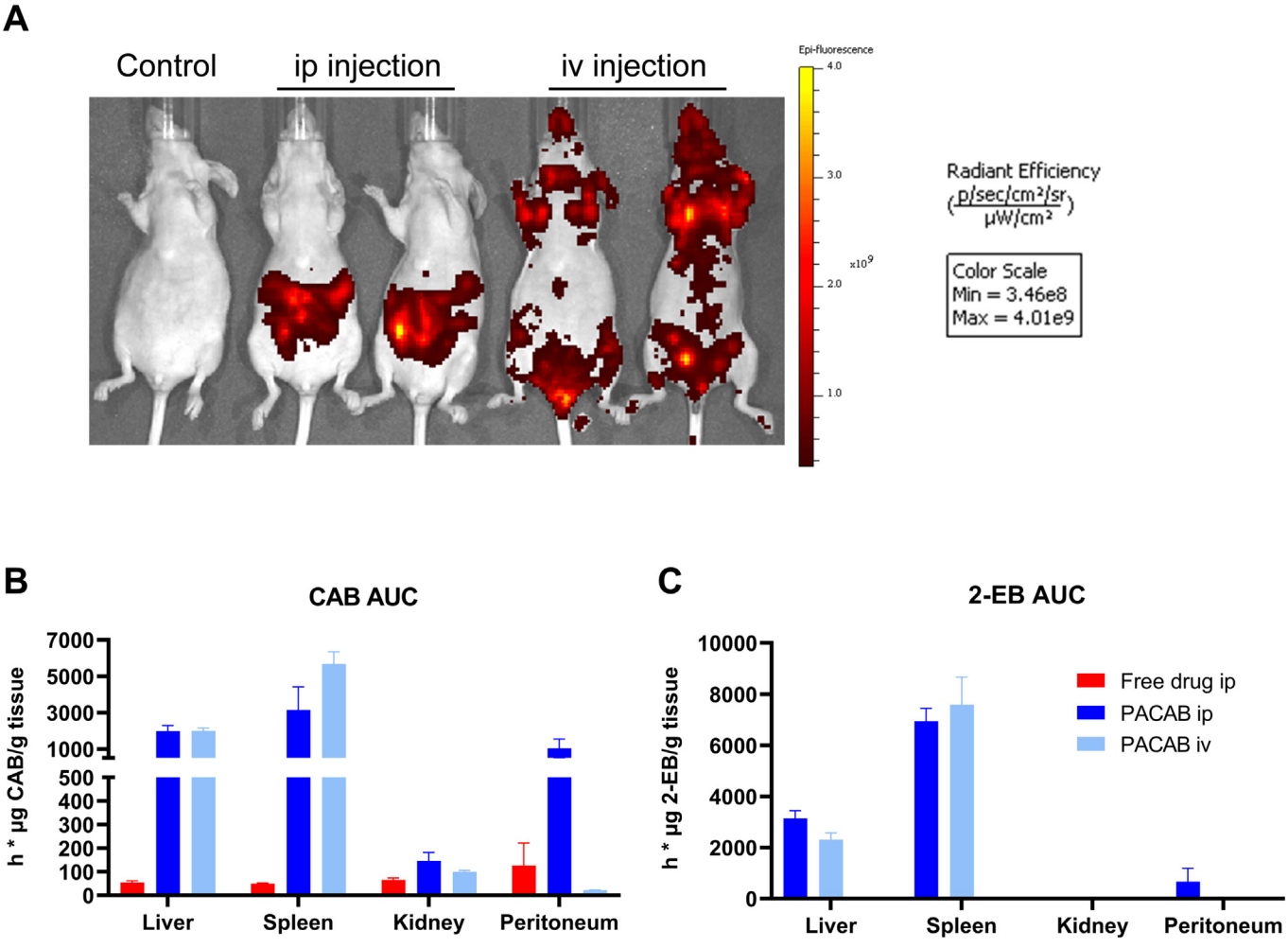

Fig. 2. A) Biodistribution of PACA-encapsulated NR668 in healthy mice. Images were obtained 1 h after injection. B–C) AUC values (1 h–35 d) of CAB (B) and 2-EB (C). Diagrams show mean values ± SD.

PACAB (6 mg CAB/kg) exhibited a similar decrease in luminescence at day 17, after which luminescence increased, indicating exponential tumor growth. Treatment with 15 mg/kg PACAB resulted in a more sustained growth inhibition compared to the other treatment groups (Fig. 5A, B). The first mice in the treatment groups reached a humane endpoint on day 38, which signifies increased survival compared to control treated animals, and all mice were euthanized at this time point to evaluate treatment response by measuring tumor weight. The mean tumor weight was 0.87 g and 0.86 g for the CAB treated

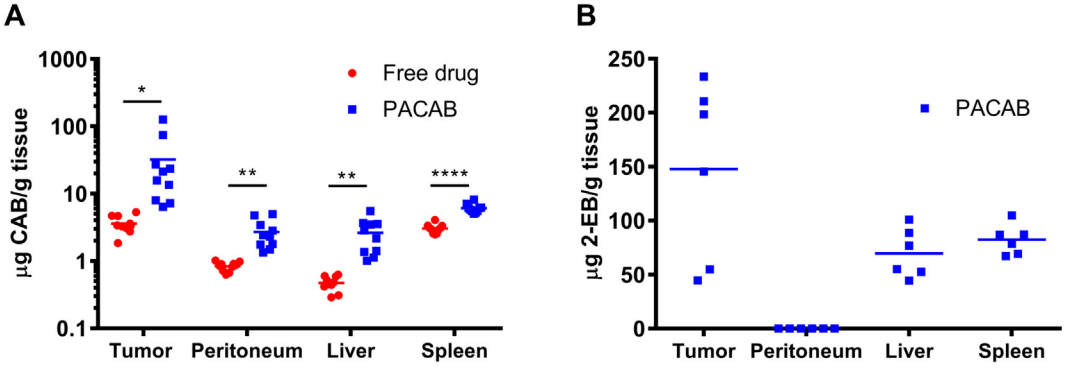

Fig. 3. Biodistribution in mice bearing B76 xenografts. A) CAB concentration on a logarithmic scale in organs harvested 2 h after ip injection of free drug (6 mg/kg) or PACAB (6 mg CAB/kg) (n = 10). B) 2-EB concentration in organs harvested 2 h after intraperitoneal injection of PACAB (6 mg CAB/kg) (n = 6). *$p < 0.05$, **$p < 0.01$, ****$p < 0.0001$.

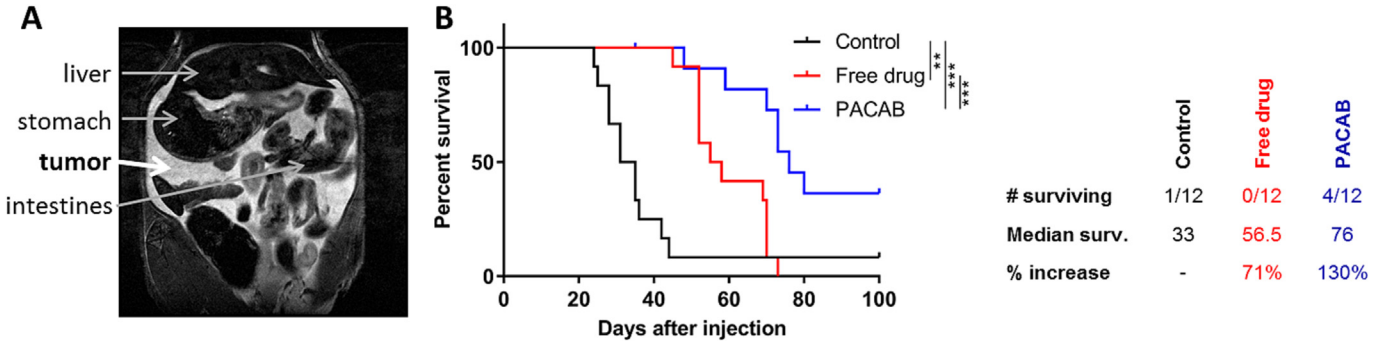

Fig. 4. Treatment efficacy of free drug and PACAB in mice bearing PMCA-3 xenografts. A) T2-weighted coronal MR image of mouse bearing PMCA-3 xenograft. The mucinous tumor tissue appears as white areas on T2-weighted images and is indicated with a white arrow. The liver, stomach and intestines are also indicated in the image with grey arrows. B) Kaplan Meier survival curve comparing animals treated with control, free drug (15 mg/kg) or PACAB (15 mg CAB/kg). The number of mice surviving to day 100, median survival (days) and % increase in survival compared to control are also shown.

groups ($p = 0.95$), while for the two PACAB treated groups, the mean tumor weights were 0.56 g and 0.15 g, respectively ($p = 0.0002$). (Fig. 5C). A significant difference in tumor weight was also observed between 15 mg/kg CAB and 15 mg/kg PACAB ($p = 0.0011$). Comparing 6 mg/kg CAB to 6 mg/kg PACAB and 15 mg/kg CAB to 6 mg/kg PACAB showed non-significant trends pointing towards differences in the favor of the PACAB groups ($p = 0.08$ and $p = 0.05$, respectively).

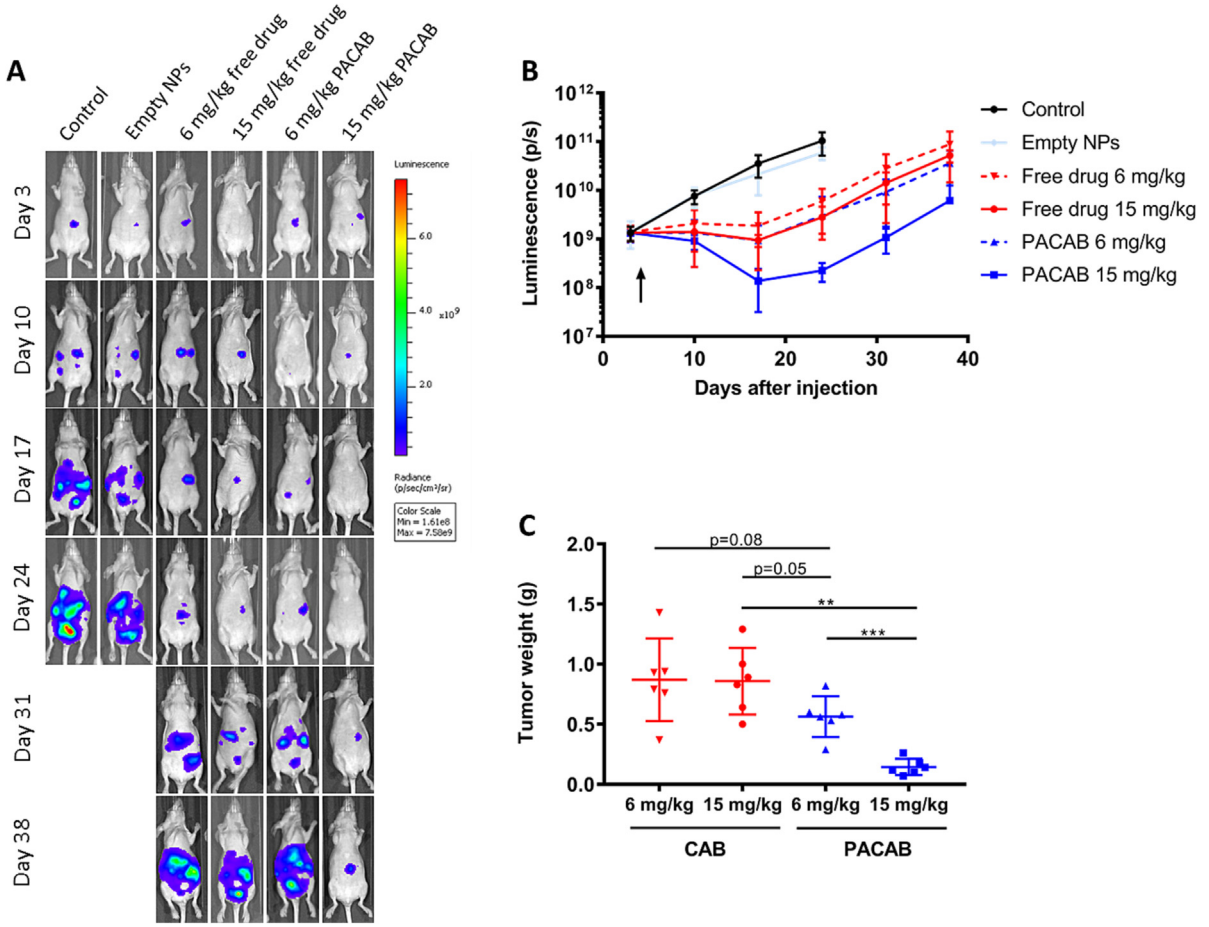

Fig. 5. Treatment efficacy of free drug and PACAB in mice bearing B76 xenografts. A) Representative IVIS images of mice injected with control solution, empty NPs, free drug or PACAB. B) Quantification of total flux luminescence (photons/second (p/s)) in B76 xenografts injected with control solution, empty NPs, free drug or PACAB. Arrow indicates treatment day. C) Tumor weight at necropsy for mice treated with free drug or PACAB. Error bars represent mean ± SD, n = 3 for empty NPs, for other groups n = 6. **p < 0.01, ***$p < 0.001$.

Discussion

A challenge with intraperitoneal administration of chemotherapy in PM is the rapid clearance of small molecule drugs, highlighting the necessity of finding methods to prolong drug retention in the peritoneal cavity to improve the treatment and survival of PM patients. The presented data shows that peritoneal retention of the cytostatic drug CAB was significantly increased by PACA NP encapsulation. This is probably partly due to a formulation-induced size increase; from free CAB having a diameter of approx. 10 nm, to PACAB with a diameter of approx. 150 nm. Small molecule drugs are easily absorbed through the peritoneal capillaries and enter systemic circulation.[5] Encapsulation within nanosized particles reduces this absorption, and the drug is therefore retained in the peritoneal cavity – resulting in increased local drug concentrations. The nanoparticles hence serve as drug depots exhibiting prolonged release kinetics and increased drug persistence at the target site.

In the presented work, a novel method for detection of NP polymeric material in biological matrices was developed. This enabled dual tracking of both the CAB drug and the NP drug carrier in different tissues. In this way, valuable information on PACAB *in vivo* biodistribution and tissue accumulation could be obtained. The peritoneal retention effect can, based on the NP biodistribution results, therefore further be explained by interactions between the NP material and intraperitoneal surfaces. This is shown by NP material content in tumor tissue and peritoneum tissue (healthy mice only). Importantly, the presented data shows that NP encapsulation significantly increases drug accumulation in tumor tissue. Different mechanisms have been suggested as possible reasons for NP selectivity to PM tumors, including physical surface interactions between NPs and tumor collagen[7] and peritoneal lymphatic flow.[8] These are primarily passive accumulation processes, enhanced by complete cavity distribution following ip injection and NP retention in the peritoneal cavity. Dual peritoneal tumor accumulation through a combination of direct local tumor penetration and indirect circulation-mediated homing, has also been reported.[7,25] Local tumor penetration is enhanced by high peritoneal drug concentrations, while circulation dependent accumulation is based on the enhanced permeability and retention (EPR) effect, describing how intravascular NPs preferentially leak into tumor tissue through the permeable tumor vasculature.[26] These reports, describing a broad variability of mechanisms, illustrate the complexity of the observed NP-tumor interaction, and may also point towards a dependency on NP material and NP physicochemical properties (*e.g.* size and charge) in addition to the tumor type. Further investigation is therefore needed to ascertain the mechanisms behind the specific PACA-tumor interaction.

The increased drug accumulation in tumor after administration of PACAB can partly explain the improved treatment response. A significant difference between PACAB and free CAB was seen in both peritoneal *in vivo* models: improved survival in the PMCA-3 and reduced growth of B76. The observed dose response in B76 tumor weight after treatment with PACAB, but not after treatment of free CAB, also highlights the beneficial effect of encapsulating the drug. In addition to the increased drug uptake in tumors caused by NPs, other mechanisms have also been suggested as possible reasons for improved treatment response by NP encapsulation. These include elevated inflammation with increased M1 macrophage infiltration,[12] or decreased levels of M2 macrophages and alteration in the microenvironment with reduced vascular endothelial growth factor-A (VEGF-A) levels.[27]

The therapeutic efficacy of PACAB and CAB was also investigated in two cell lines *in vitro*. These results show that empty NPs are non-toxic to cells at relevant therapeutic doses. No difference was observed between the PACAB and CAB groups, in line with previous results.[14,28] This shows that CAB is released from PACAB after 72 h and can exert its therapeutic activity after encapsulation. In an *in vitro* setting, the drug is not cleared by systemic circulation, hence not showing potential positive effects of NP encapsulation and retention.

Systemic exposure and damage to healthy cells is a major dose-limiting toxicity of cancer chemotherapy.[29] Although taxanes have a key role in the treatment of several malignancies, the occurrence of severe side effects, including hypersensitivity reactions, peripheral neuropathy and hematological toxicity, limit their use.[30] This challenge could be overcome by NP encapsulation of the drug.[31] In the presented toxicity study, NP encapsulation reduced the toxic burden of CAB, especially shown by a less pronounced weight reduction and fewer clinical signs (diarrhea and lack of grooming) in the PACAB group compared to the CAB group. Injection of empty NPs induced a negligible toxic effect. This is in line with the results from the initial *in vitro* toxicity study and our previous results showing that empty PACA NPs induce only mild reactions on the surface of the peritoneum, liver and kidney – where all observations were evaluated as normal effects of the ip injection and of no clinical significance.[32] All treatment groups were shown to induce significant increases in leucocyte counts, with empty NPs causing a more pronounced increase in monocyte levels compared to the CAB-treated groups. This difference in immunogenicity can be possibly be explained by the differences in the NP's chemical composition and physicochemical properties which are factors known to influence cellular responses, such as cytotoxicity, uptake rates and mode of cell death.[15,33,34] Hematology screening showed a drug-induced anemia in the CAB-treated groups – a common side effect following CAB treatment also in humans.[35] Furthermore, administration by the ip route, resulting in drug retention in the peritoneal cavity, can reduce the risk and consequences of high systemic drug concentrations. In the presented pharmacokinetic data, this was demonstrated by a significantly lower blood C_{max} value after ip administration of PACAB compared to that of iv injection of the same material.

Taxane-based chemotherapy, including CAB, paclitaxel and docetaxel, plays a major role in the management of a variety of malignancies, including ovarian, breast, prostate and lung cancers.[30,36] The clinical efficacy of taxanes can, however, be reduced by cellular resistance through the activation of the P-glycoprotein efflux pump that lowers intracellular drug concentrations through active transport.[37] While docetaxel and paclitaxel are heavily hampered by this effect, CAB is shown to have reduced affinity for the P-glycoprotein – thus reducing the possibility of drug resistance.[38] Drug resistance is further limited by NP encapsulation, which shields the drug from the efflux

transporters. Additionally, the higher lipophilicity of CAB compared to other taxanes is shown to increase blood-brain barrier crossing and to increase cell penetration through passive influx, hence leading to higher cytotoxic effects in resistant cell lines where the permeability of the plasma membrane has been altered.[39] The efficacy of CAB compared to other taxanes was exemplified by our previous studies in B76 ovarian cancer xenografts, which were insensitive to paclitaxel,[40] contrasting the strong growth inhibitory effect seen by CAB treatment. This indicates that CAB could be a good treatment alternative for patients with ovarian cancer not responding to other taxanes.

In conclusion, this work shows that encapsulation of CAB in PACA NPs increased peritoneal retention, drug uptake in tumors and improved the treatment efficacy in two *in vivo* peritoneal cancer models; an orthotopic mucinous patient-derived xenograft model and an ovarian cancer model, highlighting PACAB's efficacy and treatment potential. The promising results strongly indicate that PACAB, as a novel treatment approach for PM, could improve therapeutic outcome for a large number of patients. Based on this, a commercialization process is currently ongoing with the aim of establishing PACAB as an approved treatment for PM patients with a high unmet medical need.

Funding

This work was supported by the Research Council of Norway (309555 ENPERITO), the Research Council of Norway *via* the strategic institute project "Vivo" through the basic grants received by SINTEF Industry, the Norwegian Cancer Society (Grant No. 197837) and Astrid and Birger Torsteds legat to KGF.

CRediT authorship contribution statement

Astrid Hyldbakk: Formal analysis, Investigation, Methodology, Visualization, Writing – original draft. **Karianne Giller Fleten:** Formal analysis, Investigation, Methodology, Visualization, Writing – original draft. **Sofie Snipstad:** Formal analysis, Methodology, Writing – review & editing. **Andreas K.O. Åslund:** Formal analysis, Methodology, Writing – review & editing. **Catharina de Lange Davies:** Supervision, Writing – review & editing. **Kjersti Flatmark:** Conceptualization, Funding acquisition, Methodology, Supervision, Writing – review & editing. **Yrr Mørch:** Conceptualization, Funding acquisition, Methodology, Supervision, Writing – review & editing.

Conflict of interest

YM has patent #WO 2019/185685 pending to SINTEF TTO. YM, KF and KGF have patent #WO 2020/192950 and patent #US 16/366596 pending to SINTEF TTO.

Acknowledgements

The technical assistance of Stine Falkfjell, Maria Bratsberg Gellein, Anne Rein Hatletveit (NP synthesis and physicochemical characterization), Tonje Brunes and Stein Waagene (animal experiments) is greatly appreciated. Toxicity studies and biodistribution studies in healthy mice were conducted at the Comparative Medicine Core Facility (CoMed) at NTNU in Trondheim, Norway, where they provided housing and care of animals. Blood samples (clinical chemistry and hematology) were analyzed by the Department of Preclinical Sciences and Pathology (PREPAT) at the Norwegian University of Life Sciences. Studies in mice cancer models were performed at Department of Comparative Medicine, Oslo University Hospital. The graphical abstract was created with Biorender.com.

Appendix A. Supplementary data

Supplementary data to this article can be found online at https://doi.org/10.1016/j.nano.2023.102656.

References

1. Levine EA, Stewart JH, Shen P, Russell GB, Loggie BL, Votanopoulos KI. Intraperitoneal chemotherapy for peritoneal surface malignancy: experience with 1,000 patients. *J Am Coll Surg* 2014;**218**(4):573-85.
2. van Driel WJ, Koole SN, Sonke GS. Hyperthermic intraperitoneal chemotherapy in ovarian cancer. *N Engl J Med* 2018;**378**(14):1363-4.
3. Ceelen WP, Flessner MF. Intraperitoneal therapy for peritoneal tumors: biophysics and clinical evidence. *Nat Rev Clin Oncol* 2010;**7**(2):108-15.
4. Dakwar GR, Shariati M, Willaert W, Ceelen W, De Smedt SC, Remaut K. Nanomedicine-based intraperitoneal therapy for the treatment of peritoneal carcinomatosis - mission possible? *Adv Drug Deliv Rev* 2017;**108**:13-24.
5. Bajaj G, Yeo Y. Drug delivery systems for intraperitoneal therapy. *Pharm Res* 2010;**27**(5):735-8.
6. De Smet L, Ceelen W, Remon JP, Vervaet C. Optimization of drug delivery systems for intraperitoneal therapy to extend the residence time of the chemotherapeutic agent. Ti TK, Roncucci L, Aoyagi K, Lien HC, editors. *Sci World J* 2013;**25**720858.
7. Kim J, Shim MK, Cho YJ, Jeon S, Moon Y, Choi J, et al. The safe and effective intraperitoneal chemotherapy with cathepsin B-specific doxorubicin prodrug nanoparticles in ovarian cancer with peritoneal carcinomatosis. *Biomaterials* 2021;**279**121189.
8. Hargrove D, Liang B, Kashfi-Sadabad R, Joshi GN, Gonzalez-Fajardo L, Glass S, et al. Tumor-mesoporous silica nanoparticle interactions following intraperitoneal delivery for targeting peritoneal metastasis. *J Control Release* 2020;**328**:846-58.
9. Ando-Matsuoka R, Ando H, Abu Lila AS, Maeda N, Shimizu T, Ishima Y, et al. I.P.-injected cationic liposomes are retained and accumulate in peritoneally disseminated tumors. *J Control Release* 2022;**341**:524-32.
10. Sugarbaker PH, Stuart OA. Pharmacokinetics of the intraperitoneal nanoparticle pegylated liposomal doxorubicin in patients with peritoneal metastases. *Eur J Surg Oncol* 2021;**47**(1):108-14.
11. Couvreur P, Kante B, Roland M, Guiot P, Bauduin P, Speiser P. Polycyanoacrylate nanocapsules as potential lysosomotropic carriers: preparation, morphological and sorptive properties. *J Pharm Pharmacol* 1979;**31**(1):331-2.
12. Vauthier C. A journey through the emergence of nanomedicines with poly(alkylcyanoacrylate) based nanoparticles. *J Drug Target* 2019;**27**(5–6):502-24.
13. Merle P, Blanc JF, Phelip JM, Pelletier G, Bronowicki JP, Touchefeu Y, et al. Doxorubicin-loaded nanoparticles for patients with advanced hepatocellular carcinoma after sorafenib treatment failure (RELIVE): a phase 3 randomised controlled trial. *Lancet Gastroenterol Hepatol* 2019;**4**(6):454-65.
14. Fusser M, Øverbye A, Pandya AD, Mørch Ý, Borgos SE, Kildal W, et al. Cabazitaxel-loaded poly(2-ethylbutyl cyanoacrylate) nanoparticles improve treatment efficacy in a patient derived breast cancer xenograft. *J Control Release* 2019;**293**:183-92.

15. Snipstad S, Berg S, Mørch Ý, Bjørkøy A, Sulheim E, Hansen R, et al. Ultrasound improves the delivery and therapeutic effect of nanoparticle-stabilized microbubbles in breast cancer xenografts. *Ultrasound Med Biol* 2017;**43**(11):2651-69.
16. Snipstad S, Mørch Ý, Sulheim E, Åslund A, Pedersen A, Davies Cde L, et al. Sonopermeation enhances uptake and therapeutic effect of free and encapsulated cabazitaxel. *Ultrasound Med Biol* 2021;**47**(5):1319-33.
17. Chen Y, Pan Y, Hu D, Peng J, Hao Y, Pan M, et al. Recent progress in nanoformulations of cabazitaxel. *Biomed Mater* 2021;**16**(3)032002.
18. Sulheim E, Mørch Y, Snipstad S, Borgos SE, Miletic H, Bjerkvig R, et al. Therapeutic effect of cabazitaxel and blood-brain barrier opening in a patient-derived glioblastoma model. *Nanotheranostics* 2019;**3**(1):103-12.
19. Klymchenko AS, Roger E, Anton N, Anton H, Shulov I, Vermot J, et al. Highly lipophilic fluorescent dyes in nano-emulsions: towards bright non-leaking nano-droplets. *RSC Adv* 2012;**2**(31):11876-86.
20. Marth C, Zeimet AG, Herold M, Brumm C, Windbichler G, Müller-Holzner E, et al. Different effects of interferons, interleukin-1beta and tumor necrosis factor-alpha in normal (OSE) and malignant human ovarian epithelial cells. *Int J Cancer* 1996;**67**(6):826-30.
21. Fleten KG, Bakke KM, Mælandsmo GM, Abildgaard A, Redalen KR, Flatmark K. Use of non-invasive imaging to monitor response to aflibercept treatment in murine models of colorectal cancer liver metastases. *Clin Exp Metastasis* 2017;**34**(1):51-62.
22. Nair AB, Jacob S. A simple practice guide for dose conversion between animals and human. *J Basic Clin Pharm* 2016;**7**(2):27-31.
23. Flatmark K, Davidson B, Kristian A, Stavnes HT, Førsund M, Reed W. Exploring the peritoneal surface malignancy phenotype—a pilot immunohistochemical study of human pseudomyxoma peritonei and derived animal models. *Hum Pathol* 2010;**41**(8):1109-19.
24. Collier HO, Dinneen LC, Johnson CA, Schneider C. The abdominal constriction response and its suppression by analgesic drugs in the mouse. *Br J Pharmacol Chemother* 1968;**32**(2):295-310.
25. Simón-Gracia L, Hunt H, Scodeller PD, Gaitzsch J, Braun GB, Willmore AM, et al. Paclitaxel-loaded polymersomes for enhanced intraperitoneal chemotherapy. *Mol Cancer Ther* 2016;**15**(4):670-9.
26. Matsumura Y, Maeda H. A new concept for macromolecular therapeutics in cancer chemotherapy: mechanism of tumoritropic accumulation of proteins and the antitumor agent smancs. *Cancer Res* 1986;**46**(12 Pt 1): 6387-92.
27. Hama S, Nishi T, Isono E, Itakura S, Yoshikawa Y, Nishimoto A, et al. Intraperitoneal administration of nanoparticles containing tocopheryl succinate prevents peritoneal dissemination. *Cancer Sci* 2022;**113**(5): 1779-88.
28. Øverbye A, Torgersen ML, Sønstevold T, Iversen TG, Mørch Ý, Skotland T, et al. Cabazitaxel-loaded poly(alkyl cyanoacrylate) nanoparticles: toxicity and changes in the proteome of breast, colon and prostate cancer cells. *Nanotoxicology* 2021;**15**(7):865-84.
29. Zeien J, Qiu W, Triay M, Dhaibar HA, Cruz-Topete D, Cornett EM, et al. Clinical implications of chemotherapeutic agent organ toxicity on perioperative care. *Biomed Pharmacother* 2022;**146**112503.
30. van Eerden RAG, Mathijssen RHJ, Koolen SLW. Recent clinical developments of nanomediated drug delivery systems of taxanes for the treatment of cancer. *Int J Nanomedicine* 2020;**15**:8151-66.
31. Wang H, Yu J, Lu X, He X. Nanoparticle systems reduce systemic toxicity in cancer treatment. *Nanomedicine* 2016;**11**(2):103-6.
32. Hyldbakk A, Mørch Y, Snipstad S, Åslund AKO, Klinkenberg G, Nakstad VT, et al. Identification of novel cyanoacrylate monomers for use in nanoparticle drug delivery systems prepared by miniemulsion polymerisation - a multistep screening approach. *Int J Pharm X* 2022; **4**100124.
33. Szwed M, Sønstevold T, Øverbye A, Engedal N, Grallert B, Mørch Ý, et al. Small variations in nanoparticle structure dictate differential cellular stress responses and mode of cell death. *Nanotoxicology* 2019;**13**(6):761-82.
34. Sulheim E, Iversen TG, To Nakstad V, Klinkenberg G, Sletta H, Schmid R, et al. Cytotoxicity of poly(alkyl cyanoacrylate) nanoparticles. *Int J Mol Sci* 2017;**18**(11):2454.
35. JEVTANA® (cabazitaxel) Injection Safety Information [Internet] [Cited 2022 Nov 23]. Available from: https://www.jevtana.com/safety-information.
36. Sinha D. A review on taxanes: an important group of anticancer compound obtained from Taxus SP. *Int J Pharm Sci Res* 2020;**11**:1969-85.
37. Maloney SM, Hoover CA, Morejon-Lasso LV, Prosperi JR. Mechanisms of taxane resistance. *Cancers (Basel)* 2020;**12**(11):3323.
38. Duran GE, Derdau V, Weitz D, Philippe N, Blankenstein J, Atzrodt J, et al. Cabazitaxel is more active than first-generation taxanes in ABCB1(+) cell lines due to its reduced affinity for P-glycoprotein. *Cancer Chemother Pharmacol* 2018;**81**(6):1095-103.
39. Vrignaud P, Semiond D, Benning V, Beys E, Bouchard H, Gupta S. Preclinical profile of cabazitaxel. *Drug Des Devel Ther* 2014;**8**:1851-67.
40. Andersson Y, Haavardtun SI, Davidson B, Dørum A, Fleten KG, Fodstad Ø, et al. MOC31PE immunotoxin - targeting peritoneal metastasis from epithelial ovarian cancer. *Oncotarget* 2017;**8**(37):61800-9.